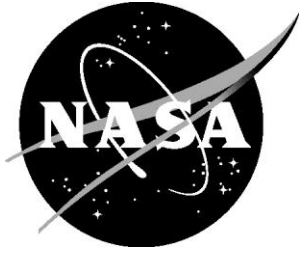# Temperature and Pressure Dependence of Signal Amplitudes for Electrostriction Laser-Induced Thermal Acoustics

*Gregory C. Herring*
*Langley Research Center, Hampton, Virginia*

May 2015

# NASA STI Program . . . in Profile

Since its founding, NASA has been dedicated to the advancement of aeronautics and space science. The NASA scientific and technical information (STI) program plays a key part in helping NASA maintain this important role.

The NASA STI program operates under the auspices of the Agency Chief Information Officer. It collects, organizes, provides for archiving, and disseminates NASA's STI. The NASA STI program provides access to the NTRS Registered and its public interface, the NASA Technical Reports Server, thus providing one of the largest collections of aeronautical and space science STI in the world. Results are published in both non-NASA channels and by NASA in the NASA STI Report Series, which includes the following report types:

- TECHNICAL PUBLICATION. Reports of completed research or a major significant phase of research that present the results of NASA Programs and include extensive data or theoretical analysis. Includes compilations of significant scientific and technical data and information deemed to be of continuing reference value. NASA counter-part of peer-reviewed formal professional papers but has less stringent limitations on manuscript length and extent of graphic presentations.

- TECHNICAL MEMORANDUM. Scientific and technical findings that are preliminary or of specialized interest, e.g., quick release reports, working papers, and bibliographies that contain minimal annotation. Does not contain extensive analysis.

- CONTRACTOR REPORT. Scientific and technical findings by NASA-sponsored contractors and grantees.

- CONFERENCE PUBLICATION. Collected papers from scientific and technical conferences, symposia, seminars, or other meetings sponsored or co-sponsored by NASA.

- SPECIAL PUBLICATION. Scientific, technical, or historical information from NASA programs, projects, and missions, often concerned with subjects having substantial public interest.

- TECHNICAL TRANSLATION. English-language translations of foreign scientific and technical material pertinent to NASA's mission.

Specialized services also include organizing and publishing research results, distributing specialized research announcements and feeds, providing information desk and personal search support, and enabling data exchange services.

For more information about the NASA STI program, see the following:

- Access the NASA STI program home page at http://www.sti.nasa.gov

- E-mail your question to help@sti.nasa.gov

- Phone the NASA STI Information Desk at 757-864-9658

- Write to:
  NASA STI Information Desk
  Mail Stop 148
  NASA Langley Research Center
  Hampton, VA 23681-2199

NASA/TM–2015-218762

# Temperature and Pressure Dependence of Signal Amplitudes for Electrostriction Laser-Induced Thermal Acoustics

*Gregory C. Herring*
*Langley Research Center, Hampton, Virginia*

National Aeronautics and
Space Administration

Langley Research Center
Hampton, Virginia 23681-2199

May 2015

## Contents

## List of Figures

**Abstract**

*The relative signal strength of electrostriction-only (no thermal grating) laser-induced thermal acoustics (LITA) in gas-phase air is reported as a function of temperature T and pressure P. Measurements were made in the free stream of a variable Mach number supersonic wind tunnel, where T and P are varied simultaneously as Mach number is varied. Using optical heterodyning, the measured signal amplitude (related to the optical reflectivity of the acoustic grating) was averaged for each of 11 flow conditions and compared to the expected theoretical dependence of a pure-electrostriction LITA process, where the signal is proportional to the square root of [P\*P /( T\*T\*T)].*

**Introduction**

Laser-induced thermal acoustics (LITA), elsewhere called laser-induced thermal grating spectroscopy (LITGS) or transient grating spectroscopy (TGS), is actively being developed [1-8] for flow measurement [9-13] including combustion applications [5, 14, 15]. Because the signals are strong, a majority of LITA efforts [5-10, 14, 15] utilize thermal gratings that are dominated by temperature gradients. Other studies [1-4, 11-13] use pure electrostriction gratings (i.e., pure acoustic waves without a thermal grating) in spite of the weaker signals. The electrostrictive approach makes the LITA technique more universal since it is a nonresonant process and does not require an absorption transition within the gas species of interest. The global collection of wind tunnels uses a variety of different working fluids, so the non-thermal-grating approach makes the use of a single instrument possible for many different flow facilities. As part of the LITA development effort at NASA Langley Research Center (LaRC), off-body flow velocity, temperature and pressure measurements were recently demonstrated [13] in a variable Mach number supersonic wind tunnel. In addition to the primary goal of proof-of-concept of LITA as a supersonic flow diagnostic, the work of [13] also makes possible the present study of the LITA signal amplitude dependence on gas density.

The signal level S of many light scattering techniques typically has either a linear or a quadratic density dependence (i.e., $S \propto P/T$ or $P^2/T^2$ respectively) for pressure P and temperature T. In contrast electrostriction-based LITA is expected [1, 16-18] to have a dependence of $S \propto P^2/T^3$. Furthermore an optically-heterodyned variation of the technique [4, 7], that mixes a local oscillator with the raw LITA signal, produces a final signal $S_h$ that varies as $S_h \propto (P^2/T^3)^{1/2} = P/T^{3/2}$. In LITA, T is readily derived from the frequency of the signal oscillations, while P is difficult to derive simultaneously from the signal decay rate at typical pressures of ~ 1 atm or smaller. Note that at larger pressures (i.e., P >> 1 atm), pressure can be derived from the decay rate as shown as shown in [15]. One potential application for amplitude measurements is to use them for an indirect pressure measurement for lower-pressure conditions. Confident knowledge of the $P^2/T^3$

relation is first necessary to infer pressure from measurements of T and S when P is not easily measured from the decay rate.

Grating time decay [8, 15, 19] and pressure dependence of LITA signal amplitudes [1, 15 20] have been studied in some detail, but there are few studies of the pure temperature dependence. One study [16] that reports a temperature dependence of $T^3$ uses raw data that has roughly a factor-of-three noise superimposed on the temperature trend. This naturally leads to a desire for better data to confirm this temperature dependence with better accuracy. The lack of other studies investigating the temperature dependence motivated the present effort in this report to compare the previously-measured LITA signal variation with theory. The work of Reference 13 was originally intended to measure only Mach number and temperature of the wind tunnel flow, but after publication of Reference 16, it was natural to ask how the signal amplitudes of [13] vary with P and T, since the noise of [13] was less than the noise of [16].

In this report, the theoretical dependence on pressure P and temperature T is compared to data previously [13] obtained in the NASA Langley Unitary Plan Wind Tunnel (UPWT). Ideally, P and T would be varied independently as in [1, 16, 20] to check the P and T dependencies. However in the UPWT, P and T cannot be varied independently because they were forced to vary simultaneously as the wind tunnel Mach number M was changed by varying the nozzle expansion ratio. Thus instead of looking for a pure $T^3$ dependence at constant P in the current work, the dependence of the LITA signal is studied when changing P and T simultaneously. Fortunately the flow conditions P and T are both known with confidence [21].

**Method and Apparatus**

Two common-path versions of optical-heterodyne LITA, from LaRC, were described for subsonic ($V_F < V_S$) [4] and supersonic ($V_F > V_S$) [13] fluid motion at velocity $V_F$ and sound speed $|\pm V_S| = V_S$. Two crossed beams from a single 10-nsec pulsed laser (pump) electrostrictively create two counter propagating 1-μsec duration acoustic plane wave packets in the medium volume defined by the beam crossing (30 Hz repetition rate). The volume of the ellipsoidal overlap region is about 1 cm by 200 μm by 200 μm. For stationary or subsonic gas, illumination of these traveling wave packets (i.e., density gratings) with a second laser beam (probe) at frequency $\Omega_L$ that crosses the initial density-grating ellipsoid and generates a Bragg-diffracted signal laser beam that consists of two copropagating components that are spectrally distinct. These two components are distinguished by their different Doppler shifts $\pm \Delta\omega$ determined by the counter propagating geometry of the two acoustic wave packets. The beating of the two separate components, at frequencies $\Omega_L \pm \Delta\omega$, produces a modulation of this Bragg-diffracted signal beam at frequency $2\,\Delta\omega$. If the sound wave reciprocal wavelength is $\Delta k$ (i.e., wave vector difference of the two pump beams), the two Doppler shifts are $\Delta\omega = \mathbf{\Delta k} \bullet (\pm\mathbf{V_S})$, where $\pm\mathbf{V_S}$ are the velocities of the two counter propagating wave packets and $|\pm\mathbf{V_S}|$ = the speed of sound (bold-faced quantities denote vectors).

Measurement of the beat frequency $2\,\Delta\omega$, with the known grating wavelength $1/\Delta k$, yields the sound speed. If the mass composition of the fluid is known, translational temperature is determined since $T \propto V_S^2$. Any non-zero bulk fluid motion at velocity $V_F$ is also readily obtained from LITA with a heterodyne [10-12] approach. A local oscillator beam at the probe frequency $\Omega_L$ is introduced onto the detector. The local oscillator mixes nonlinearly with the original signal, and the detected signal then shows modulation at three frequencies: $2\,\Delta\omega$ and $\Delta\omega \pm (\Delta\mathbf{k} \bullet \mathbf{V}_F)$. $V_F$ is derived from the measured frequency difference, $2\,\Delta\omega'$, of the two new components, where $\Delta\omega' = \Delta\mathbf{k} \bullet \mathbf{V}_F$. The signal is digitized, and the frequencies can be extracted by a variety of methods to determine the velocity and temperature of the fluid. The fluid pressure can also be determined with LITA from decay rates of either thermal [15] or electrostriction [13] grating signals.

For supersonic gas flow, the subsonic setup was modified by offsetting the probe beam $X_o \approx 0.25$ mm downstream of the crossed pumps to optimize collection of the reflected light signals from the two acoustic Bragg gratings as they are swept downstream. (Note that this present estimate of $X_o \approx 0.25$ mm is more accurate than the previous estimate of $X_o \approx 0.5$ mm given in Reference 13, which was specified only to describe the experimental setup. The value 0.5 mm was not used in Reference 13 to derive the relative pressures reported in that work, but the value 0.25 mm is used in the present work to calculate the absorption of the acoustic wave packets.) A schematic of the supersonic version of LITA is shown in Figure 1. Measurements were made in the UPWT, a large-scale (1.3 by 1.3-meter test section) closed-circuit supersonic facility that has been widely used for 50 years [21]. Mach number was varied over 11 values from 1.47 to 2.16 to give 11 different combinations of P and T.

Offsetting the probe laser beam downstream relative to the crossed pumps slightly changes the temporal profile of the LITA signal. A fast acoustic wave packet travels at Mach number M+1 and a slower packet travels at M-1 in the detector reference frame. For each laser pulse the diffracted signal consists of two components (one from each grating) that are separated in time by about 500 ns. Each of the two components exhibits a different characteristic frequency due to distinct Doppler shifts. In the analysis presented here, the total LITA signal S is taken as the sum of these two sequential signals. Each single-pulse waveform was first Fourier transformed to frequency domain. Then about 500 spectra were averaged. In this analysis, the raw amplitudes are corrected for transit time and absorption effects. Finally the amplitudes of the two separate signals (from the fast and slow acoustic wave packets) were added together to generate the final initial signal amplitude $S_h$ for each different P and T combination.

**Results**

Writing the non-heterodyned LITA signal as $S \propto g(P, T)$ where g is a function of P and T, four choices of g are considered: $g \propto P/T$, $g \propto P^2/T^2$, $g \propto P^4/T^4$, and $g \propto P^2/T^3$, which correspond to linear, quadratic, and quartic density dependences, and the expected LITA dependence respectively. For $g = f^2$ and heterodyned LITA signals $S_h$, these dependences become $S_h \propto f \propto (P/T)^{1/2}$, $f \propto P/T$, and $f \propto (P/T)^2$ and $f \propto P/T^{3/2}$

respectively. Figure 2 shows calculated results for the reduction of the heterodyned signal as a function of Mach number (i.e., P and T are both decreasing with increasing M) for the four different choices of function f. The present measured fractional changes in signal amplitudes $dS_h/S_h$ are also shown by individual filled-circle symbols. These 15 measurements covering 11 Mach numbers are from the same 15 runs presented in Reference 13, where M, P and T were reported (but the signal amplitudes were not reported). Two flow conditions were repeated and the precision of the amplitude $S_h$ of each point is estimated to be about $\pm$ 30% from these limited repetitions.

The same data as shown in Figure 2 are plotted in a different manner in Figure 3, where the fractional theoretical signal is plotted versus the fractional change in observed signal. One expects an equality $df/f = dS_h/S_h$ (i.e., linear relation with slope = 1), for the correct theoretical dependence on P and T. The expected equality is shown with the solid line in each plot.

Results of linear fitting to the four comparisons of Figure 3 are shown in Table 1, where all uncertainties are 68% confidence (i.e. $\pm$ 1$\sigma$). Note that the fitted lines through the data sets are not shown in Figure 3. The results of the linear fitting are shown only in Table 1. The solid lines of Figure 3 are not fits; they simply show the equality $df/f = dS_h/S_h$. At face value, the slope for $f \propto P/T$ (i.e. $S \propto P^2/T^2$ which is quadratic with density) is closest to unity and the only slope consistent with unity at 68% confidence. The other three options are also ruled out at 95% confidence ($\pm$ 2$\sigma$).

**Discussion and Summary**

First the spread in the data of the present work is about $\pm$30%, much less than the factor-of-three spread in the data of Reference 16. Unfortunately, the changes in P and T for the present work are less than the factor-of-three change in temperature used in Reference 16. Thus the sensitivity to temperature of the current study in is probably not better than the sensitivity of Reference 16.

Since optical heterodyne detection was used in the work of [13], $f \propto P/T^{3/2}$ is the expectation for a physical process like LITA with a straightforward, non-heterodyned dependence $S \propto P^2/T^3$. However, in Figure 2, the function $f \propto P/T$ best matches the data compared to the other options. Also, in Figure 3 and Table 1, the same function is also the best match to the equality between $df/f$ and $dS_h/S_h$, with a unity slope. Because of the significant spread in the data and the uncertainties in the fitted slopes, the function $f \propto P/T^{3/2}$ is also plausibly consistent with the data, but on face value, comes in second place to the best match, $f \propto P/T$. The two functions $f \propto (P/T)^{1/2}$ and $f \propto P^2/T^2$ are not consistent with the data to 95% confidence.

The bottom line is that, in this work, $f \propto P/T$ provides a better match than $f \propto P/T^{3/2}$ for the UPWT data set. Theoretically [1, 18], $S \propto P^2/T^3$ (i.e., $S_h \propto f \propto P/T^{3/2}$) is expected. The first possible conclusion is that LITA signals vary as $S \propto P^2/T^2$, i.e. density squared, and not as $P^2/T^3$ as reported in the literature. This conclusion is difficult to accept based on the literature, including the $1/T^3$ measurement result of Reference 16.

Note that the heat capacity ratio and the Gladstone-Dale coefficient are both required to be temperature independent to get the $P^2/T^3$ result. But these assumptions should be relatively good approximations for the pressures and temperatures of this work. A second possible conclusion is that there is an error in the present analysis. Note that Reference 17 reports a decay of electrostriction gratings faster than $1/T^3$ (i.e., $1/T^{4.25}$) and discusses possible effects from turbulent convection, beam steering, and averaging with non-linear effects. In the present work, the observed decay is slower than $1/T^3$. Other possibilities for errors in the present work are related to the pump-probe laser beam separation $X_o$ and imperfect beam alignments. Finally an incorrect result may be due to systematic errors in the absorption estimate (between the time of formation and the time of measurement of the density gratings) in the data analysis.

On the other hand, the absorption calculation is the same one that allowed the correct determinations of the wind tunnel free-stream relative pressures to within $\pm 4\%$ in Reference 13. This argues that the absorption calculation is likely to be reasonable and that there may be other unknown systematic errors in the present analysis. Because of the potential errors in the present experiment and the $1/T^3$ result of Reference 16, it is reasonable to continue to assume that $S \propto P^2/T^3$ is correct. With respect to the pressure measurement method proposed above in the introduction, significantly better data than those used in [13] or [16] must be obtained before the amplitude dependence on temperature can be confirmed accurately enough to provide confidence in future measurements of S to be used as an indirect pressure probe in gas samples, with pressures near atmospheric or below.

## Acknowledgement

## References

1. D. E. Govoni, J. A. Booze, A. Sinha, and F. F. Crim, "The nonresonant signal in laser-induced grating spectroscopy of gases," Chem. Phys. Lett. **216**, 525-529 (1993).

2. W. Hubschmid, B. Hemmerling, and A. Stampanoni-Panariello, "Rayleigh and Brillouin modes in electrostrictive gratings," J. Opt. Soc. Am. B **12**, 1850–1854 (1995).

3. A. Stampanoni-Panariello, B. Hemmerling, and W. Hubschmid, "Electrostrictive generation of non-resonant gratings in the gas phase by multimode lasers," Phys. Rev. A **51**, 655–662 (1995).

4. R. C. Hart, G. C. Herring, and R. J. Balla, "Common-path heterodyne laser-induced thermal acoustics for seedless laser velocimetry," Opt. Lett. **27**, 710-712 (2002).

5. S. Williams, L. A. Rahn, P. H. Paul, J. W. Forsman, and R. N. Zare, "Laser-induced thermal grating effects in flames," Opt. Lett. **19**, 1681–1683 (1994).

6.  M. A. Buntine, D. W. Chandler, and C. C. Hayden, "Detection of vibrational overtone excitation in water via laser-induced grating spectroscopy," J. Chem. Phys. **102**, 2718–2726 (1995).

7.  A. A. Maznev, K. A. Nelson, and J. A. Rogers, "Optical heterodyne detection of laser-induced gratings," Opt. Lett. **23**, 1319-1321 (1998).

8.  E. B. Cummings, H. G. Hornung, M. S. Brown, and P. A. DeBarber, "Measurement of gas-phase sound speed and thermal diffusivity over a broad pressure range using laser-induced thermal acoustics," Opt. Lett. **20**, 1577–1579 (1995).

9. D. J. W. Walker, R. B. Williams, and P. Ewart, "Thermal grating velocimetry," Opt. Lett. **23**, 1316–1318 (1998).

10.  S. Schlamp, E. B. Cummings, and T. H. Sobota, "Laser-induced thermal-acoustic velocimetry with heterodyne detection," Opt. Lett. **25**, 224-226 (2000).

11.  B. Hemmerling, D. N. Kozlov, and A. Stampanoni-Panariello, "Temperature and flow velocity measurements by use of laser-induced electrostrictive gratings," Opt. Lett. **25**, 1340-1342 (2000).

12.  R. C. Hart, R. J. Balla R J, and G. C. Herring, "Simultaneous velocimetry and thermometry of air by use on nonresonant heterodyned laser-induced thermal acoustics," Appl. Opt. **40**, 965-968 (2001).

13.  R. C. Hart, G. C. Herring, and R. J. Balla, "Pressure measurement in supersonic airflow by differential absorptive laser-induced thermal acoustics," Opt. Lett. **32**, 1689-1691 (2007).

14.  M. S. Brown and W. L. Roberts, "Single-point thermometry in high-pressure, sooting, premixed combustion environments," J. Propulsion Power **15**, 119-127 (1999).

15.  R. Stevens and P. Ewart, "Simultaneous single shot measurement of temperature and pressure along a one dimensional line by use of laser-induced thermal grating spectroscopy," Opt. Lett. **31**, 1055-1058 (2006).

16.  A. Meier, and S. Schlamp, "Improved signal intensity for transient grating spectroscopy using a PIV laser," AIAA 36th Fluid Dynamics Conference, San Francisco, CA (June 5-8, 2006) paper 2006-2973.

17.  S. Schlamp, R. T. Rosgen, D. N. Kozlov, C. Rakut, P. Kasal, and J. von Wolferdorf, "Transient grating spectroscopy in a hot turbulent compressible free jet," J. Propulsion Power **21**, 1008-1018 (2005).

18. R. J. D. Miller, R. Casalegno, K. A. Nelson, and M. A. Fayer, "Laser-induced ultrasonics: a dynamic holographic approach to the measurement of weak absorptions, optoelastic constants and acoustic attenuation," Chem. Phys. **72**, 371-379 (1982).

19. Y. Li, W. L. Roberts, and M. S. Brown, "Investigation of acoustic gaseous damping rates by transient grating spectroscopy," AIAA Journal **40**, 1071-1077 (2002).

20. F. Bake and F. Lehmann, "Preliminary investigations on thermometry in thermal flows via transient grating spectroscopy," 12th International Symposium on Applications of Laser Techniques to Fluid Mechanics, Lisbon, Portugal (July 12-15, 2004) paper 12.4

21. C. M. Jackson Jr., W. A. Corlett, and W. J. Monta "Description and calibration of the Langley unitary plan wind tunnel," NASA TP-1905 (November 1981).

**Table 1**

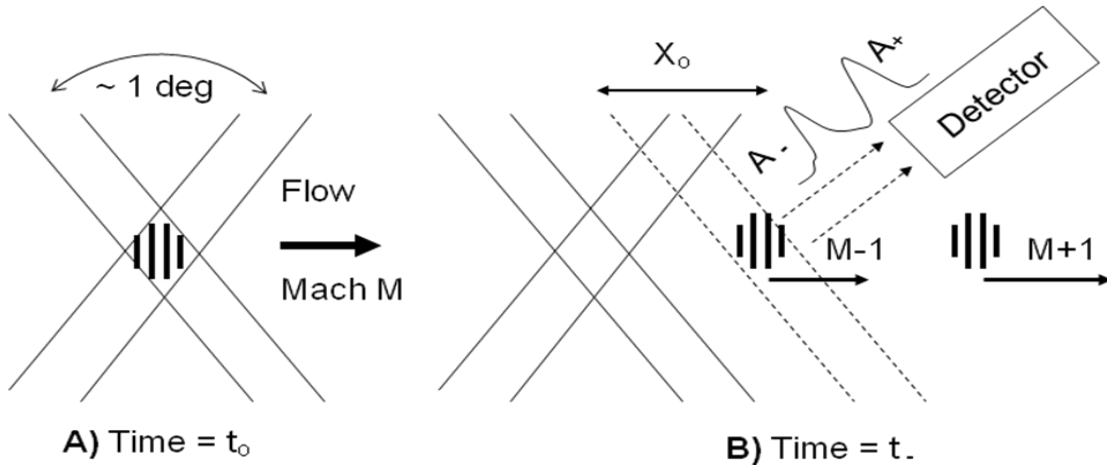| Function  g | Function  f | Slope | Intercept | $R^2$ |
|---|---|---|---|---|
| $P^4/T^4$ | $P^2/T^2$ | $2.7 \pm 0.35$ | $0.015 \pm 0.13$ | 0.82 |
| $P^2/T^2$ | $P/T$ | $1.01 \pm 0.12$ | $0.028 \pm 0.05$ | 0.83 |
| $P^2/T^3$ | $P/T^{3/2}$ | $0.65 \pm 0.08$ | $0.02 \pm 0.03$ | 0.83 |
| $P/T$ | $(P/T)^{1/2}$ | $0.44 \pm 0.05$ | $0.017 \pm 0.02$ | 0.84 |

Figure 1. Schematic of (A) pump beam crossing geometry at the grating formation time $t_o$ and (B) a short time later $t_-$ after the two gratings (thick vertical lines) have propagated downstream and the slower grating is reflecting a fraction (i.e. signal A-) of the probe beam (dashed lines) into the detector [probe beam and detector are omitted from part (A) for clarity].
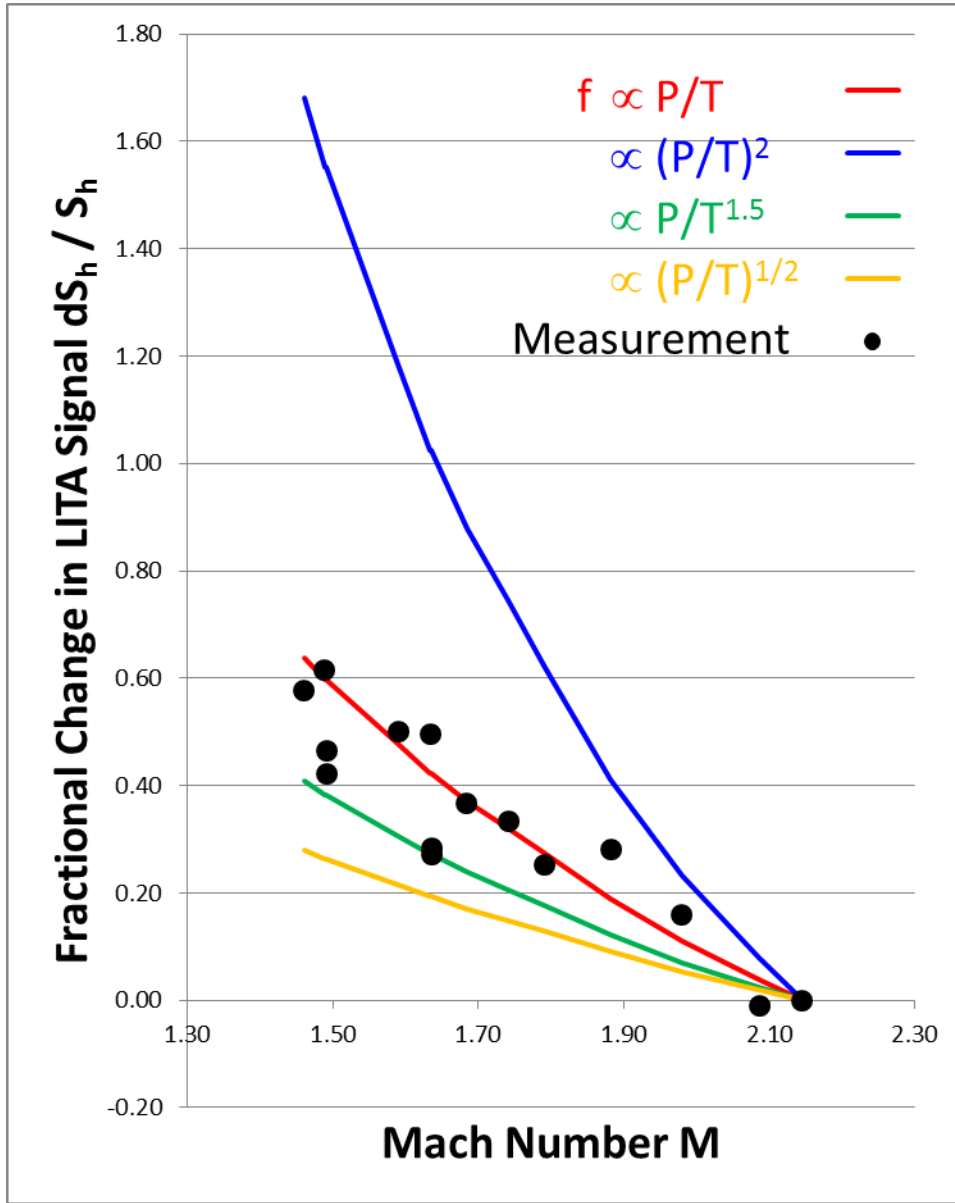
Figure 2. Relative decrease in heterodyned LITA signal $S_h$ as a function of increasing Mach number for four different functional dependences f of pressure P and temperature T and the measurements from the UPWT [13].
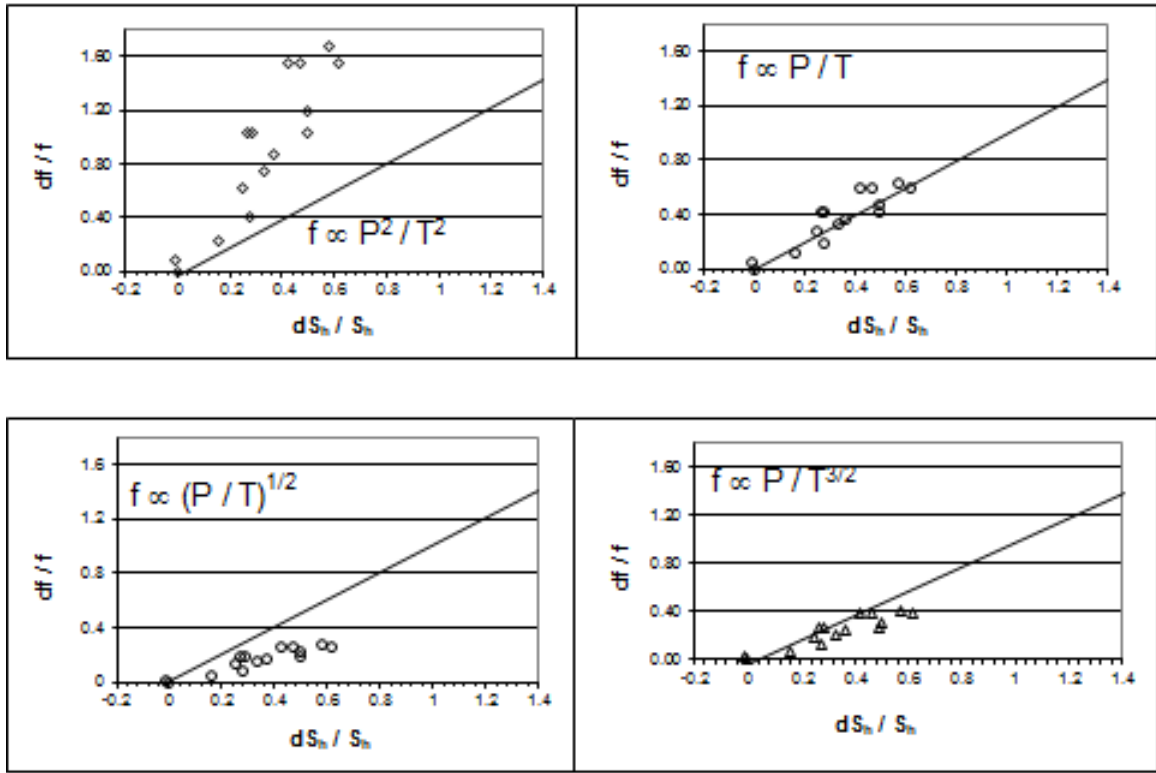
Figure 3. Fractional change in theoretical df/f versus the fractional change in observed heterodyned signal $dS_h / S_h$ for the four different P and T dependences denoted on each panel.

# REPORT DOCUMENTATION PAGE

*Form Approved*
*OMB No. 0704-0188*

The public reporting burden for this collection of information is estimated to average 1 hour per response, including the time for reviewing instructions, searching existing data sources, gathering and maintaining the data needed, and completing and reviewing the collection of information. Send comments regarding this burden estimate or any other aspect of this collection of information, including suggestions for reducing this burden, to Department of Defense, Washington Headquarters Services, Directorate for Information Operations and Reports (0704-0188), 1215 Jefferson Davis Highway, Suite 1204, Arlington, VA 22202-4302. Respondents should be aware that notwithstanding any other provision of law, no person shall be subject to any penalty for failing to comply with a collection of information if it does not display a currently valid OMB control number.
**PLEASE DO NOT RETURN YOUR FORM TO THE ABOVE ADDRESS.**

| 1. REPORT DATE *(DD-MM-YYYY)* | 2. REPORT TYPE | 3. DATES COVERED *(From - To)* |
|---|---|---|
| 01- 05 - 2015 | Technical Memorandum | |

**4. TITLE AND SUBTITLE**

Temperature and Pressure Dependence of Signal Amplitudes for Electrostriction Laser-Induced Thermal Acoustics

**5a. CONTRACT NUMBER**

**5b. GRANT NUMBER**

**5c. PROGRAM ELEMENT NUMBER**

**6. AUTHOR(S)**

Herring, Gregory C.

**5d. PROJECT NUMBER**

**5e. TASK NUMBER**

**5f. WORK UNIT NUMBER**

794072.02.07.07.01

**7. PERFORMING ORGANIZATION NAME(S) AND ADDRESS(ES)**

NASA Langley Research Center
Hampton, VA 23681-2199

**8. PERFORMING ORGANIZATION REPORT NUMBER**

L-20562

**9. SPONSORING/MONITORING AGENCY NAME(S) AND ADDRESS(ES)**

National Aeronautics and Space Administration
Washington, DC 20546-0001

**10. SPONSOR/MONITOR'S ACRONYM(S)**

NASA

**11. SPONSOR/MONITOR'S REPORT NUMBER(S)**

NASA-TM-2015-218762

**12. DISTRIBUTION/AVAILABILITY STATEMENT**

Unclassified - Unlimited
Subject Category36
Availability: NASA STI Program (757) 864-9658

**13. SUPPLEMENTARY NOTES**

**14. ABSTRACT**

The relative signal strength of electrostriction-only (no thermal grating) laser-induced thermal acoustics (LITA) in gas-phase air is reported as a function of temperature T and pressure P. Measurements were made in the free stream of a variable Mach number supersonic wind tunnel, where T and P are varied simultaneously as Mach number is varied. Using optical heterodyning, the measured signal amplitude (related to the optical reflectivity of the acoustic grating) was averaged for each of 11 flow conditions and compared to the expected theoretical dependence of a pure-electrostriction LITA process of heterodyned signal is proportional to the square root of [P*P /( T*T*T)].

**15. SUBJECT TERMS**

Electrostriction; Grating reflectivity; Laser-induced thermal acoustics; Pressure; Temperature dependence of laser-induced; Transient grating supectroscopy

| 16. SECURITY CLASSIFICATION OF: | | | 17. LIMITATION OF ABSTRACT | 18. NUMBER OF PAGES | 19a. NAME OF RESPONSIBLE PERSON |
|---|---|---|---|---|---|
| a. REPORT | b. ABSTRACT | c. THIS PAGE | | | STI Help Desk (email: help@sti.nasa.gov) |
| U | U | U | UU | 17 | 19b. TELEPHONE NUMBER *(Include area code)* (757) 864-9658 |

**Standard Form 298** (Rev. 8-98)
Prescribed by ANSI Std. Z39.18